Studies of the interaction between human and viral proteins

Viveka Ramaiah

Degree project in applied biotechnology, Master of Science (2 years),
2012 Examensarbete i tillämpad bioteknik 30 hp till masterexamen,
2012
Biology Education Centre and Department of Medical Biochemistry and Microbiology, IMBIM, BMC, Uppsala University
Supervisors: Per Jemth and Celestine Chi

TABLE OF CONTENTS:

Abstract:

Human papillomavirus is an oncovirus whose transforming activity is exhibited through one of its early protein in its genome called E7 in combination with E6. p21 is a tumor suppressor protein which inhibits cyclin dependent kinase activity arresting the cells in the S phase. E7 protein reverse the cyclin dependent kinase inhibitory effect of p21 through binding with the carboxy terminus of p21 allowing the cells to enter into the S phase. Inorder to block HPV E7 protein during infection it is important to understand the molecular mechanism of binding interaction between E7 and p21. To assess binding mechanism of interaction we have performed kinetic studies of E7 and p21. We cloned and expressed wildtype and mutants of HPV E7 and p21. Affinity purification followed by anion exchange and reverse phase chromatography gave the required pure protein for stability and binding studies. Stability studies were performed for the respective proteins by monitoring far UV circular dichroism and tryptophan fluorescence. The stability experiments of the protein purified with and without urea suggested that both approaches yielded well-folded HPV E7. The binding studies performed between HPV16 E7 and p21 wildtypes at different temperatures revealed that the binding exhibited a biphasic kinetic behaviour.

Abbrevations:

ACN- Acetonitrile

CDKs- Cyclin- dependent kinases

DMSO- Dimethyl sulfoxide

dNTP- Deoxyribonucleotide triphosphate

IMAC- Immobilized metal ion affinity chromatography

IPTG- Isopropyl β-D-1-thiogalactopyranoside

MES- 2-(*N*-morpholino)ethanesulfonic acid

PCR- Polymerase chain reaction

PCNA- Proliferating cell nuclear antigen

RB- Retinoblastoma protein

TFA- Trifluoroacetic acid

SDS PAGE- Sodium dodecyl sulfate polyacrylamide gel electrophoresis

1. Introduction:

1.1. HPV:

Human papillomaviruses (HPVs) belong to the oncovirus type having transforming capacity, for example by integrating the viral genome within the host cell's DNA following their entry into the host cell (3). HPV is an oncogenic double stranded DNA virus, causing infections in skin and mucosal regions. It is the causative agent of cervical cancer, a type of carcinoma responsible for more than 80 percent of the cancer deaths in women worldwide (4). There are more than 100 types of HPV strains found and among them 40 are associated with genital infections (5). HPV infecting genital areas are classified into high and low risk types (6). High risk types include HPV 16, 18, 31, 33, 35, 39, 45, 51, 52, 56 and 58. High risk types affect genitals and may lead to cervical cancer. Low risk types includes HPV 6, 11, 40, 42, 43, 44, 53, 54, 61, 72, 73, 81 and they generally cause genital infection but do not result in tumor progression (6 & 7).

1.2. HPV Genome:

The HPV genome is 8 kilo base pairs in size. It includes three different regions: a long control region (1kb) which does not code for any protein, with two other regions (early (4kb) and late genes (3kb)) coding for early and late proteins (8). The early proteins E1, E2, E4, and E5 play a vital role in genome replication and transcription. E6 and E7 are oncoproteins involved in transformation and are located in the nucleus (Figure 1). The late proteins L1 and L2 contribute to the viral capsid coat during virion formation (9).

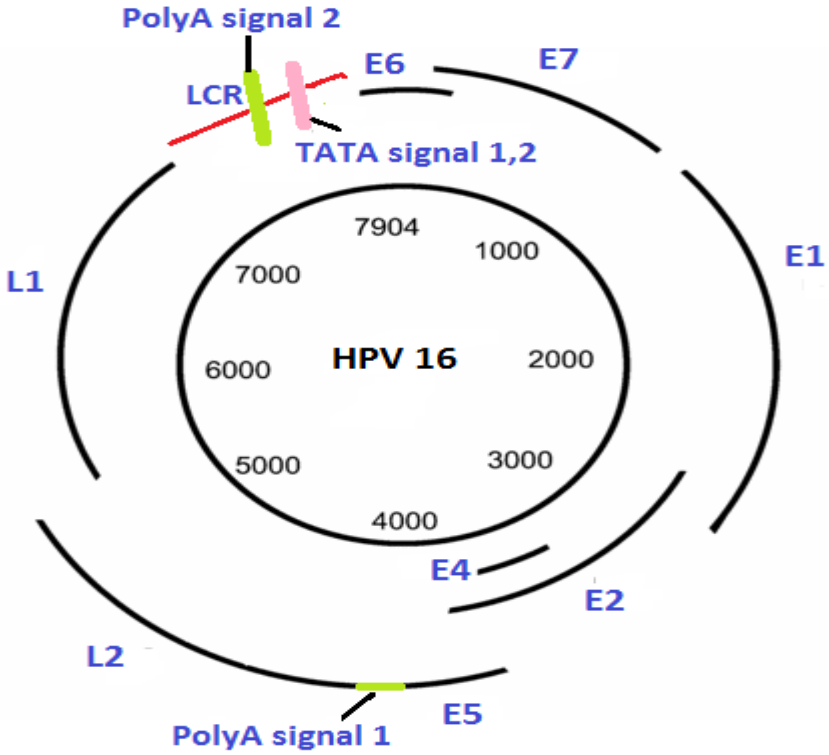

Figure 1. HPV16 genome showing the arrangement of early and late genes in its genome. It shows the early genes E1, E2, E4, E5, E6 and E7 followed by the late genes L1 and L2. The poly signal and TATA signal sequences are present between the early and late genes. Adapted from ref. 4.

1.3. HPV infection and tumor formation:

Prior to HPV infection, the virus enters the cells of stratified squamous epithelium. Integration of the viral genome occurs at the frail sites of the host genome disrupting major portion of the viral genome (10). The viral genome integration results in maintaining the stability of mRNAs of the early proteins involved in transformation (11). E6 and E7 oncoproteins maintain the transformation activity of viral genome resulting in tumor formation (12). HPV interacts with the cell cycle machinery through two ways. In one way E7 protein interacts with pRb resulting in activation of E2F, affecting the expression of the proteins required for DNA replication of the host cell and causing an unchecked S phase. The other way is through E6 binding to p53 making p53 non-functional so that DNA damage repair mechanism is affected and overriding the G_1-S phase check point (10). During a cell division, a cell goes through the interphase and mitosis. Interphase includes 3 stages, G1 phase where cells increase in size synthesizing proteins and enzymes required for DNA replication, S phase in which DNA replication occurs and G2 phase where the cell growth is completed so that the cell is ready to enter the mitosis. Two important check points G_1-S and G_2-M are involved in regulation of the normal cell cycle. p53 and Rb are the important regulatory elements which monitors the cell control check points. Alteration in the regulatory genes would lead to genetic instability resulting in tumor formation (1).

1.4. E7 motifs:

E7 has three conserved regions, CD1, CD2 and CD3. The CD1 region cannot bind with retinoblastoma protein (pRb), whereas E7 N terminal region contains LXCXE motif binding pRb at the CD2 region (15). E7 binding to the pRb affects the binding of pRb to E2F transcription factor (14). Other than pRb, E7 also binds to inhibitors of CDK, p21 and p27. These binding events result in the prevention of the host cell entering the S phase required for normal cell cycle (16, 17). E7 consists of 98 aminoacids with C terminal region containing two Cys-X-X-Cys motifs that are required for zinc ion coordination at the CD3 region (Figure 2). The C terminal zinc binding motif present in the CD3 region is capable of interacting with pRb and p21(18, 19).

1.5. E7 domains in transformation:

The transformation potential of HPV16 E7 is influenced by the pRb binding region of the CD2 domain in the N terminal portion. Mutational studies suggested that replacing the aminoacids 16-30 in the region responsible for pRb binding in the HPV16 E7 with the aminoacids from the low risk strain HPV6 E7 which has no transformation potential resulted in loss of transformation activity (17). The CD3 domain which is responsible for zinc binding has been shown to be associated with transformation (19).

1.6. p21:

p21 is a tumor supressor protein required for G_1 to S phase entry, regulating tumor growth through its interactions with cyclin A and cyclin E (21). p21 is involved in binding with CDK inhibitor at the N-terminal domain of cyclins and CDK-binding motifs (20,21,22). p21 inhibits cyclin dependent kinase, arresting the cells in G1 phase (Figure 2) (23,24). The N terminal region of E7 contains the binding site for cyclins and CDK. The C terminal portion has a second binding site for cyclins and for the proliferating cell nuclear antigen (PCNA) (25,26,27). p21 has been indicated to be involve in events of cell cycle progression, replication and DNA repair mechanism (28,29). The E7 protein reverses the cyclin dependent kinase inhibitory effect of p21 through binding with the carboxy terminus of p21 allowing the

cells to enter the S phase (30). The cyclin dependent kinase inhibitory activity of p21 is blocked on interacting with HPV16 E7 (31).

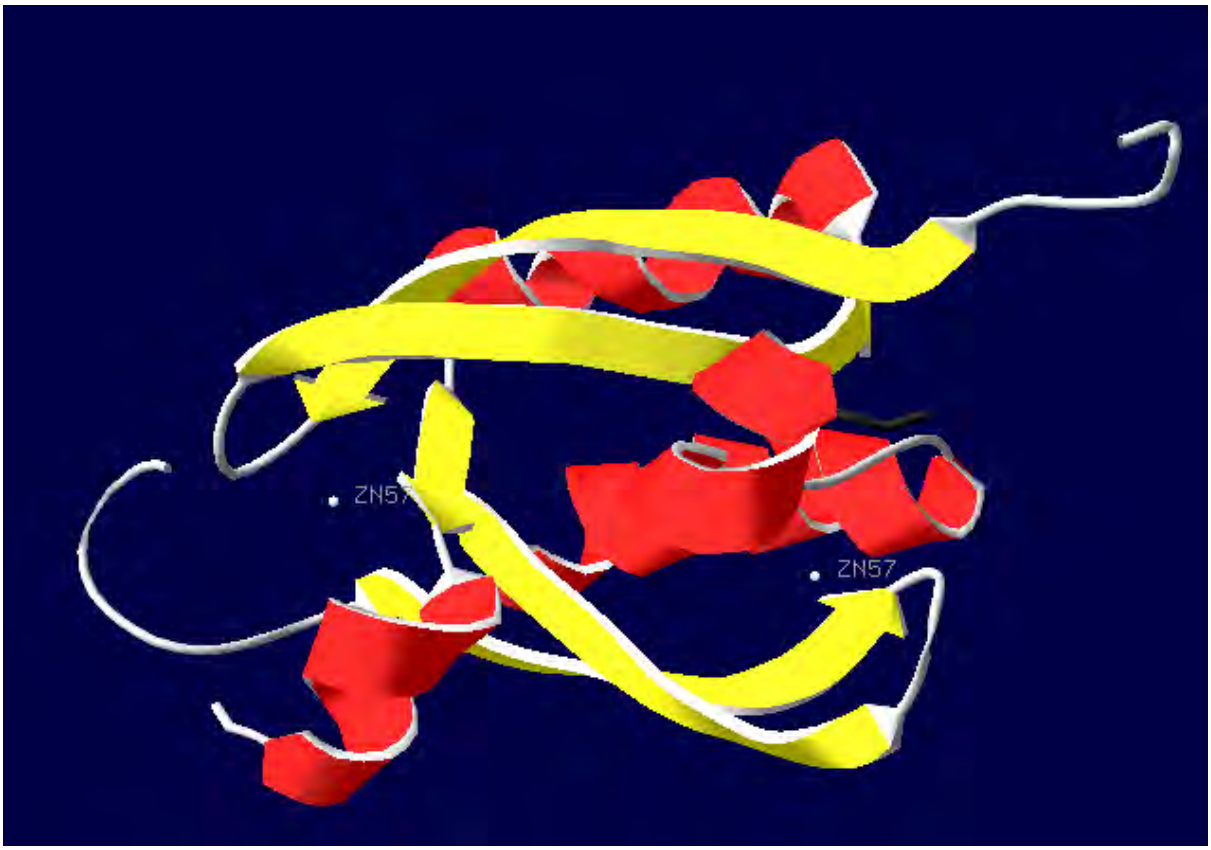

Figure 2: NMR structure of HPV45 E7 C terminal domain dimer. The helices are represented in red and the strands in yellow. The helices and strands are interconnected through loops which are shown in the figure. Zinc ions are labelled in the figure. PDB ID-2F8B.

1.7. Background information on the methods used for stability and binding studies:

1.7.1. Fluorimetry:

Fluorescence is a property in which the analyte molecules are excited at one particular wavelength and emits at a different wavelength. By monitoring the emission spectrum, information can be obtained both qualitatively and quantitatively regarding the analyte molecule. When a molecule is excited, it absorbs energy which causes it to be in the excited state which has higher energy level and it has to come to the ground state *i.e.* lower energy level. The difference in the energy level is emitted as fluorescence spectra at one particular wavelength on the basis of the energy gap between ground state and excited state. Fluorescence spectroscopy is widely used to study protein folding, unfolding by monitoring the changes in fluorescence for the aromatic aminoacid tryptophan. In case of protein studies, fluorescence is used to check the changes in the environment of tryptophan aminoacid residues. The denaturation can be caused in a protein by increasing the temperature or adding a chemical reagent for example urea or GdnHCl. Protein denaturation causes a red shift in the emission if the tryptophan residue buried in the hydrophobic core region is exposed to the hydrophilic solvent (33).

1.7.2. Circular dichroism:

Circular dichroism is based on the principle of differential absorption of the two different components *i.e.* L, left handed and R, right handed of the plane polarised light being passed through prism. The difference in absorption is generated as circular dichroism spectra in terms of ellipticity as a function of wavelength. Circular dichroism spectra can be used in analysis of both nucleic acids and proteins. In protein studies it is used to find the percentage of helices, sheets and loops of the secondary structure of protein (far UV CD spectrum), protein tertiary structure (near UV CD spectrum), thermal stability of the protein secondary and tertiary structure, etc. By monitoring the melting curve i.e. far UV CD obtained by varying the temperature at a particular wavelength in which the change in secondary structure can be predicted *i.e.* 210 nm, it is possible to determine whether the protein gets unfolded by following the change in secondary structure (31).

1.7.3. Stopped flow spectroscopy:

In order to measure the binding kinetics, the molecules containing probes to monitor the spectral property change during binding must be quickly mixed. A regular spectrometer lacks this rapid mixing process. Hence stopped flow instrument is developed which offers very fast mixing in milliseconds and also favors the usage of extrinsic probes attached to the protein for binding studies. Usually one molecule contains fluorescent moiety to act as probe. The molecule containing a fluorescent group is mixed with another molecule. The solution is mixed quickly in milliseconds as it enters the reaction cell, then the fluorescence change occurs because of binding. The kinetic data obtained through the binding reaction is fitted to the respective equation depending upon the binding behaviour. For example in case of biphasic kinetic behaviour exhibited during binding then the kinetic trace would be fitted to the double exponential equation:

$$A=\Delta A_{\mathbf{Eq}}(1-e^{-kobs1t})+\Delta B_{\mathbf{Eq}}(1-e^{-kobs2t})+C \quad \text{- - ->Equation 1}$$

where A is the signal measured with time t; $\Delta A_{\mathbf{Eq}}$ and $\Delta B_{\mathbf{Eq}}$ are amplitudes of the corresponding phases; and k_{obs} is the observed rate constant. The observed rate constant values for the fast phase were then fitted to the general equation for reversible association of two molecules which binds together.

The general equation for observed rate constant is

$$k_{obs} = (k^2_{on0})^2 + k^2_{off} + 2k_{on}k_{off}(n+\text{?}_0))^{0.5} \text{ --->Equation 2}$$

where k_{on} is the association or on-rate constant, k_{off} is the dissociation or off rate constant, (A_o) and n are the initial concentrations of the binding molecules (34).

2. Aim:

In order to understand ways of blocking HPVE7 protein during infection it is important to dissect the molecular mechanism of E7-p21 interaction. Thus the aim of this study is to understand the biophysical aspects of E7 protein interacting with p21. Therefore we attempted to

- Clone, express and purify HPV16 E7, HPV45 E7 wild types and the mutants.
- Clone, express and purify the C-terminal domain of p21(p21C) (residues 149-164) wildtype and its mutant.
- Determine the stability of E7 by denaturation through chemical denaturant guanidine hydrochloride and temperature.
- To perform binding experiments between E7 and p21C at different temperatures.

3. Material and Methods:

3.1. Cloning:

Wild type constructs encoding the HPV proteins HPV16 E7F, (full length E7 from HPV 16 amino acid residues 1-103), HPV45 E7F (full length E7 from HPV45 aminoacid residues 1-106) and tumor supressor protein p21F (full length p21 residues 1-164), p21C (aminoacid residues 149-164) were amplified by PCR and subcloned into the BamHI and EcoRI sites of pRSETA vector (Invitrogen) either with an N-terminal lipoyl domain with a thrombin cleavage site and a histidine tag attached to it (MHHHHH-lipo-LVPRGS) i.e. for HPV16 E7F, p21F and p21C or with a short his tag attached to the N-terminal (MHHHHH-LVPRGS) i.e. for HPV45 E7F. Mutations were then introduced in the conserved residues (87, 90, 98, 101) and non conserved residues (78, 91) that were present at the interface and that formed a part of the E7 dimer based on the available information from HPV11 E7 protein crystal structure (PDB code 2ewl). Mutations involving tryptophan amino acid W101V in HPV45 E7 (to remove its fluorescence) and Y151W in p21 were made to act as a probe to monitor binding during stopped-flow fluorimetry and equilibrium studies. For PCR reactions contents and cycles refer to Appendix I and II. The product of the PCR reaction was checked on 1% agarose gel in 1x TBE buffer (45 mM Tris- borate, pH 8.0, 1 mM EDTA (ethylene diamine tetra acetic acid). Successful PCR products were then digested with 0.5 µl Dpn I (Stratagene), and transformed into *E.coli* XL1 blue (Stratagene). For transformation, 2 µl of plasmid DNA was added to 50 µl of the competent *E.coli* XL1 cells. The XL1 cells containing the plasmid DNA was then incubated in ice for 30 minutes followed by a heat shock at 42^0C for 45 seconds then followed incubation on ice for 2 minutes. 200 µl of the LB media was then added to the cells and grown at 37^0C for 30 minutes in a rotary shaker. The cells were then plated on LB agar plates containing 100 µg/ml ampicillin followed by overnight incubation. A single colony was picked from the plates, grown in LB and purified using Omega Biotek kit following the manufacturing protocol. The presence of the mutation was confirmed by sequencing (Uppsala genome center, Uppsala University). The sequenced samples were referred to as clones.

The primers used in mutating HPV45 E7 and p21 wild types were as follows:

HPV45 E7 Mutation:

HPV45 E7-T76A

Forward:ggc aga att gag ctt **gca** gta gag agc tcg gca

Reverse: tgc cga gct ctc tac tgc aag ctc aat tct gcc

HPV45 E7-E78A

Forward:att gag ctt aca gta **gcg** agc tcg gca gag gac

Reverse:gtc ctc tgc cga gct cgc tac tgt aag ctc aat

HPV45 E7-L87N

Forward:gag gac ctt aga aca **aac** cag cag ctg ttt ttg

Reverse:caa aaa cag ctg ctg gtt tgt tct aag gtc ctc

HPV45 E7-L90Q

Forward:aga aca cta cag cag **cag** ttt ttg agc acc ttg

Reverse:caa ggt gct caa aaa ctg ctg ctg tag tgt tct

HPV45 E7-F91Y

Forward:aca cta cag cag ctg **tat** ttg agc acc ttg tcc

Reverse:gga caa ggt gct caa ata cag ctg ctg tag tgt

HPV45 E7-V98W/ W101V

Forward:acc ttg tcc ttt **ttg** tgt ccg **gtg** tgt gca act aac

Reverse:gtt agt tgc aca cac cgg aca caa aaa gga caa ggt

HPV45 E7-W101V

Forward:tcc ttt gtg tgt ccg **gtg** tgt gca act aac caa

Reverse:ttg gtt agt tgc aca cac cgg aca cac aaa gga

p21 Mutation:

p21-Y151W

Forward:agc atg aca gat ttc **tgg** cac tcc aaa cgc cgg

Reverse:ccg gcg ttt gga gtg cca gaa atc tgt cat gct

3.2. Expression and Purification:

The clones were expressed in *E.coli* BL21(DE3)pLysS strain (Invitrogen). The plasmid containing the desired cDNA was transformed and grown on an LB plate containing 100 µg/ml of ampicillin and 35 µg/ml of chloramphenicol. A few colonies were used to inoculate a 10 ml culture containing 100 µg/ml of ampicillin, 35 µg/ml of chloramphenicol and grown for 3 to 4 hours at 37^0C. A large scale culture of 1L containing LB and ampicillin 50ug/ml was then inoculated and the cells were grown at 37^0C up to an A_{600} of 0.8. Protein expression was induced by adding isopropyl-β-D-thiogalactopyranoside (IPTG) to a final concentration of 1 mM. Expression was done overnight at 18^0C. Cells were harvested by centrifugation and the pellet was resuspended in a buffer containing 50 mM Tris HCl, pH 7.4, 400 mM NaCl, 20 mM Imidazole, 2 mM mercaptoethanol. Cells were lysed by sonication and centrifuged at 37000 g for one hour. The supernatant of the sonicated sample was collected and filtered using 0.45 µm and 0.22 µm filters respectively. The filtered fraction was then subjected to Immobilized metal ion affinity chromatography (IMAC) Sepharose FF (Amersham Biosciences) charged with nickel. Equilibration and washing were done using the same buffer (50 mM Tris HCl, pH 7.4, 400 mM NaCl, 20 mM imidazole, 2 mM mercaptoethanol). Partially pure proteins were eluted in 250 mM Tris HCl, pH 8 and 2 mM mercaptoethanol in aliquotes of 8 ml. The dialyzed IMAC fractions of HPV45E7 and its mutants were purified using the Q sepharose column equilibrated with 20 mM MES pH6.0, 1 mM mercaptoethanol. Elution was done with a gradient from 0-2 M NaCl in 20 mM MES pH 6.0, 1 mM mercaptoethanol. The dialyzed fractions of HPV16 E7F, Lipo-p21 and mutants of Lipo-p21 were then digested with 20 units of thrombin (Amersham Biosciences) and were again allowed to pass through the nickel column equilibrated with 50 mM Tris HCl, pH 7.4, 400

mM NaCl, 20 mM imidazole, 2 mM mercaptoethanol and the peptide fraction was collected as a flow through. The lipo part of the protein was eluted with 250 mM Tris HCl, pH 8 and 2 mM mercaptoethanol. The flow through fractions of protein from the IMAC of constructs HPV16 E7F, p21 and its mutants were subjected to reversed phase chromatography on a C18 column, which was equilibrated with 0.1% TFA and developed with a gradient of 0-100% acetonitrile containing 0.1% TFA.

3.3. Protein identity confirmation:

Fractions containing the pure protein were then checked on SDS PAGE stained with Coomassie brilliant blue (See Appendix III for gel and stain composition). The identity of the protein was confirmed using matrix assisted laser desorption ionization time of flight mass spectrometry. The protein concentration was determined by measuring the absorbance at 280 nm and by dividing the absorbance with the extinction coefficient calculated using the ProtParam web tool (http://web.expasy.org/protparam/) for the respective protein. Ake Engstrom did the mass spectrometry analysis.

3.4. Binding studies:

HPV16 E7F and p21C binding kinetics were performed using an SX-20MV stopped-flow spectrometer (Applied Photophysics, Leatherhead, UK) at 37^0C and 10^0C in either 50 mM potassium phosphate at pH 6.2 and/or pH 7.4 respectively. To find the rate constants for the binding, the p21C concentration was varied and HPV16 E7F was maintained to be constant (1 μM). Equal volumes of HPV16 E7F and p21C were mixed rapidly in the stopped flow instrument using two different syringes. The binding was monitored and the kinetic traces of HPV16 E7F and p21C binding were then fitted to a double exponential function (equation 1) since biphasic kinetic behaviour was found to be exhibited during the binding. The general equation of a bimolecular association (equation 2) was used to find the on and off rate constants of binding.

3.5. Stability Studies:

Stability studies were done for the native HPV16 E7F, HPV16 E7F purified with 4 M urea as well as for HPV45 E7F and HPV45 E7C. Denaturation experiments were done in 50 mM potassium phosphate, pH 7.4 at 25^0C. Guanidine hydrochloride buffer was prepared using 7 M GdnHCl in 50 mM potassium phosphate. Stability measurements were carried using 3 μM protein with 7 M GdnHCl as the highest concentration of the GdnHCl. It was followed by a stepwise increase in addition of the GdnHCl buffer for denaturing the protein. The experiment was performed on an SLM 4800 spectrofluorimeter (SLM Instruments). Excitation was done at 280 nm and emission measured between 300-500 nm. Measured fluorescence intensity was plotted against GdnHCl concentration and fitted into solvent denaturation equation (32):

□=*(*□N+□N[denaturant] + (□D+□D[denaturant]) exp [□D-N([denaturant]–[D] 50%)/RT]/ (1+exp [□D-N ([denaturant] – [D] 50%)/RT]). equation. 3
Where F is the measured fluorescence signal
$□_N$ and □ are intercepts of native and denatured state
$□_N$ and $□_D$ are slopes of the fitted base lines
[mD-N] is the constant of proportionality with units of cal/mol/M (energy/M).
(D) 50% is the concentration of the denaturant in which 50% of the protein is denatured.

Far UV circular dichroism studies were done on a Jasco J-810 Spectropolarimeter for HPV45

E7F, HPV45 E7C and p21C. Before turning on the instrument nitrogen gas was used to flush the lamp for 10 minutes. The temperature controller and the water bath were turned on. After initializing the instrument, the shutter and the lamp was then turned on. The lamp is warmed up prior to sample introduction for almost an hour. 600 µl of the protein sample was placed into the cuvette, and CD signals were recorded between 200 and 260 nm at 25^0C. 25 µM protein in 50 mM potassium phosphate, pH 7.5 were used for analysis of HPV45 E7F, HPV45 E7C and p21C. CD spectra were obtained as the molar ellipticity of the protein recorded as a function of the wavelength. For melting studies of the protein E7F, 25 µM HPV45 E7F in 50 mM potassium phosphate, pH 7.5 was used and the temperature was gradually increased from 4^0C till 90^0C and CD signal was recorded at a particular wavelength i.e. 210 nm.

4. Results:

4.1. Cloning:

Mutants of HPV45 E7F, HPV45 E7C, p21C and p21F were amplified at 62^{o}C by PCR reaction (Figure 3) and cloned into the pRSETA vector with an N-terminal His tag attachment for HPV45 E7 constructs and with a lipoyl domain and a thrombin digestion site for p21 constructs. Mutants of HPV45 E7C and p21C were amplified at 60^{o}C, 61^{o}C, 62^{o}C and 64^{o}C respectively by PCR and cloned into the pRSETA vector with an N-terminal His tag for HPV45 E7C and with a lipoyl domain containing thrombin site for p21C (Figure 4).

4.1.1. Agarose gel analysis of PCR samples of plasmid pRSETA containing DNA fragments *i.e.* HPV45 E7C, HPV45 E7F, p21C and p21F mutants:

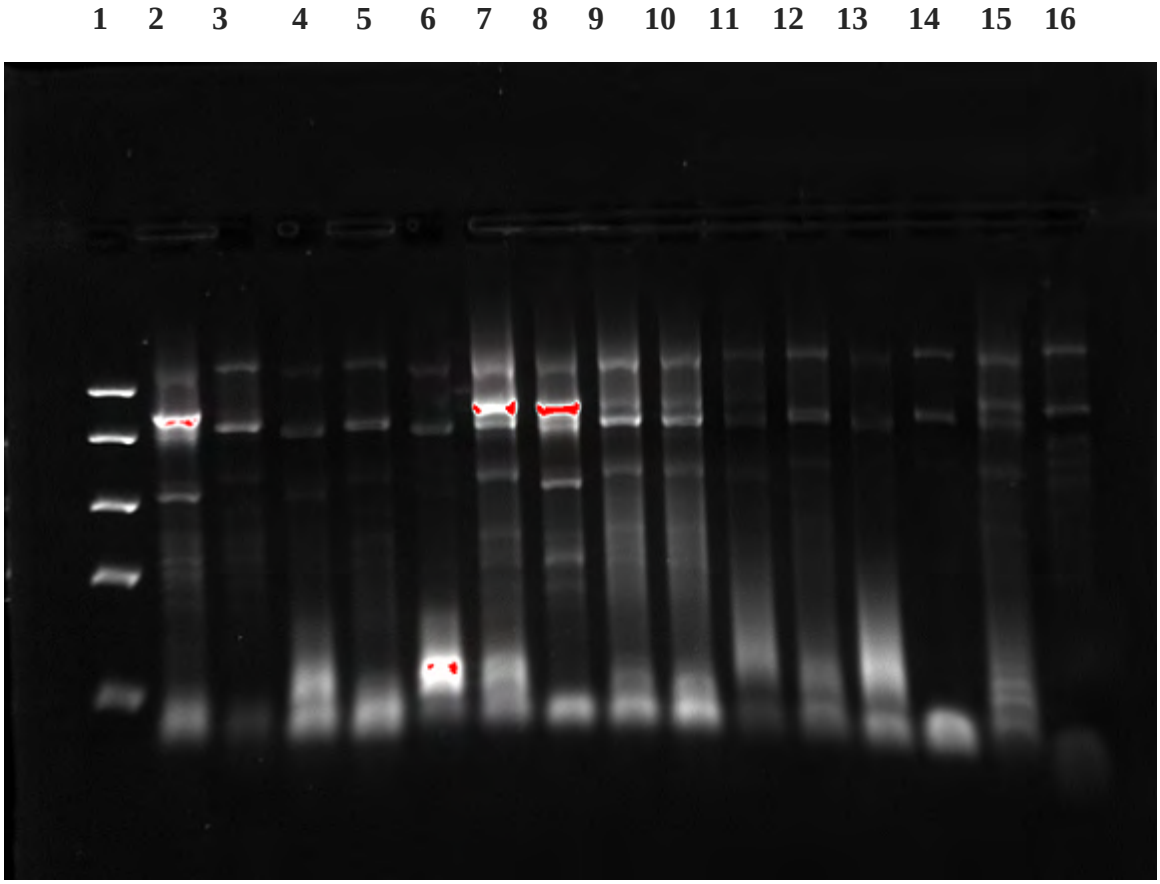

Figure 3. Electrophoresis of plasmid pRSETA fragments carrying the desired gene of interest obtained by site directed mutagenesis through PCR in nondenaturing agarose gel. The lanes are represented as Lane 1: marker (1 kb DNA ladder); Lane 2: E7CT76A; Lane 3: E7FT76A; Lane 4: E7CE78A; Lane 5: E7FE78A; Lane 6: E7CL87N; Lane 7: E7FL87N; Lane 8: E7CL90Q; Lane 9: E7FL90Q; Lane 10: E7FF91Y; Lane 11: E7CW101V; Lane 12: E7FW101V; Lane 13: E7CY98W/W101V; Lane 14: E7FY98W/W101V; Lane 15: p21CY151W; Lane 16: p21FY151W. The samples are electrophoresed on 1X TBE, 1% agarose gel with gel red as the intercalating agent (agarose with TBE buffer, gel red in the ratio 10000:1, v/v). C stands for carboxy terminal sequence and F for full length sequence.

4.1.2. Agarose gel analysis of PCR samples of plasmid pRSETA containing DNA *i.e.* HPV45 E7C and p21C mutants:

1 2 3 4 5 6 7 8 9 10 11 12 13 14

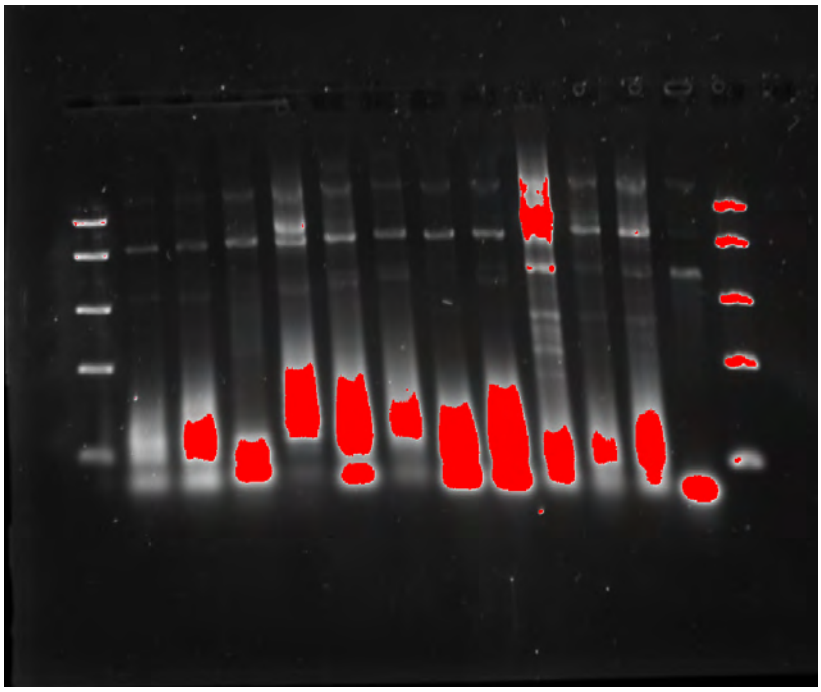

Figure 4. Electrophoresis of plasmid pRSETA fragments carrying the desired gene of interest obtained by site directed mutagenesis through PCR was performed in nondenaturing agarose gel. The lanes are represented as Lane 1- Marker (1 kb DNA ladder), Lane 2- E7CE78A (60^{o}C), Lane 3- E7CE78A (64^{o}C), Lane 4- E7CL87N (60^{o}C), Lane 5- E7CL87N (64^{o}C), Lane 6- E7CW101V (60^{o}C), Lane 7- E7CW101V (64^{o}C), Lane 8- E7CY98W/W101V (60^{o}C), Lane 9- E7CY98W/W101V (64^{o}C), Lane 10- p21CY151W (60^{o}C), Lane 11- p21CY151W (61^{o}C) , Lane 12- p21CY151W (62^{o}C), Lane 13- p21CY151W (64^{o}C), Lane 14- Marker (1kb DNA ladder). The samples are electrophoresed on 1X TBE, 1% agarose gel with gel red as the intercalating agent (agarose with TBE buffer, gel red in the ratio 10000:1, v/v). C stands for carboxy terminal sequence and F for full length sequence.

4.2. Expression and Purification:

The cloned constructs, namely wild types of HPV16 E7F, HPV45 E7F, HPV45 E7C and p21C, mutants of HPV45 E7F and HPV45 E7C were chosen for expression and purification studies. The protein expression of wild types was higher compared to their corresponding mutants in case of HPV45 E7F and p21C (Figure 5 & 6). The expressed proteins were subjected to partial purification through IMAC. In case of p21C, thrombin was added to digest the protein after IMAC purification to yield the p21C peptide to be suitable for reverse phase purification to get purity of higher order (Figure 9). Since the protein got precipitated after thrombin digestion, 3 M urea was added to purify it before loading it onto the reverse phase column (Figure 5). The separation of p21C peptide from the lipo part of the protein after thrombin digestion is confirmed through mass spectroscopy analysis of the reverse phase chromatography sample (Figure 11 & 12). The wild type of HPV45 E7F was subjected to anion exchange chromatography to obtain higher purity (Figure 10) and the collected fractions showing protein peaks in the chromatogram was checked for protein presence

through SDS PAGE. The protein got precipitated; hence 4 M urea was used for purification before loading it into the Q column (Figure 6). The mutant of HPV45 E7C *i.e.* L90Q was purified using anion exchange chromatography and the purity of the protein was checked through SDS PAGE (Figure 7). Reversed phase chromatography was performed for the tryptophan mutant of p21C *i.e.* Y151W inorder to separate the peptide fragment from the lipo part (Figure 8). The final concentration of the protein was found to be 250 μM for p21C and 88 μM for HPV16 E7F.

4.2.1. SDS PAGE analysis of the sonication and purified IMAC fractions of wild type p21C and HPV45 E7F:

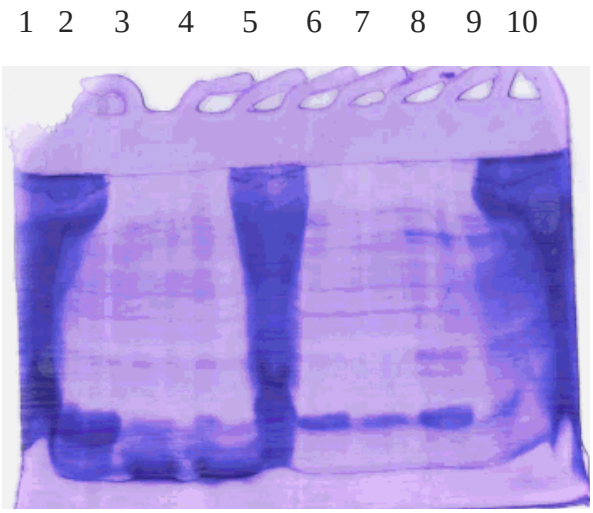

Figure 5. The sonicated and purified fractions of p21C and HPV45 E7F wild types were subjected to 15% sodium dodecylsulfate polyacrylamide gel under reducing conditions. The lanes are represented as Lane 1- p21C wild type sonicated, Lane 2- p21C wildtype IMAC, Lane 3- p21C wildtype thrombin digested, Lane 4- p21C wildtype thrombin + urea, Lane 5- HPV45 E7F wildtype sonicated, Lane 6- HPV45 E7F wildtype IMAC, Lane 7- HPV45 E7F wildtype IMAC, Lane 8- HPV45 E7FT76A IMAC, Lane 9- HPV45 E7FL87N IMAC, Lane 10- HPV45 E7FL87N sonicated. The slab gel was stained with Coomassie Blue R250 and destained with acetic acid : isopropanol : water (1:1:10, v/v).

4.2.2. SDS PAGE analysis of purified IMAC fractions of p21C, HPV45 E7C mutants and anion exchange samples of HPV45 E7F wild type:

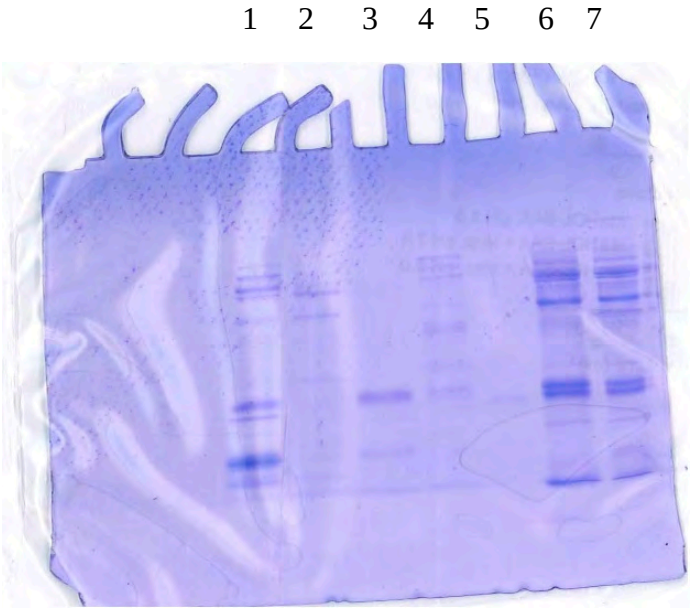

Figure 6. The purified IMAC fractions of p21C, HPV45 E7C mutants and anion exchange samples of HPV45 E7F wild type were subjected to 15% sodium dodecylsulfate polyacrylamide gel under reducing conditions. The lanes are represented as: Lane 1: p21CY151W IMAC; Lane 2: HPV45 E7F wild type (27); Lane 3: HPV45 E7F wild type (11 & 12); Lane 4: HPV45 E7F wild type (24); Lane 5: HPV45 E7F wild type (12); Lane 6: HPV45 E7CW101 IMAC boiled; Lane 7: E7CW101 IMAC. The numbers in paranthesis indicates the fractionation tube number of protein elution. The slab gel was stained with Coomassie Blue R250 and destained with acetic acid: isopropanol: water (1:1:10, v/v).

4.2.3. SDS PAGE analysis of IMAC fractions of HPV45 E7F wild type, HPV45 E7C mutant, p21C wild type and anion exchange results for HPV45 E7C L90Q:

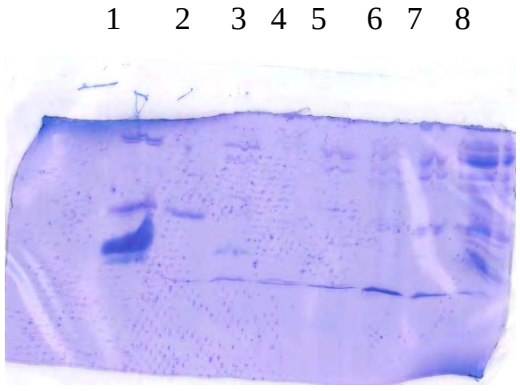

Figure 7. IMAC fractions of HPV45 E7F wildtype, HPV45 E7C mutant, p21C wild type and anion exchange fractions of HPV45 E7C L90Q were subjected to 15% sodium dodecylsulfate polyacrylamide gel under reducing conditions. The lanes are represented as Lane 1: HPV45 E7F wild type IMAC; Lane 2: HPV45 E7C W101V IMAC; Lane 3: HPV45 E7C L90Q (12-14); Lane 4: HPV45 E7C L90Q (15-16); Lane 5: HPV45 E7C type (16); Lane 6: HPV45 E7C wild type (18); Lane 7: HPV45 E7C wild type (21); Lane wild 8: p21C wildtype IMAC. The number in paranthesis indicates the fractionation tube number of protein elution. The slab gel was stained with Coomassie Blue R250 and destained with acetic acid: isopropanol: water (1:1:10, v/v).

4.2.4. Reversed phase chromatography of p21CY151W:

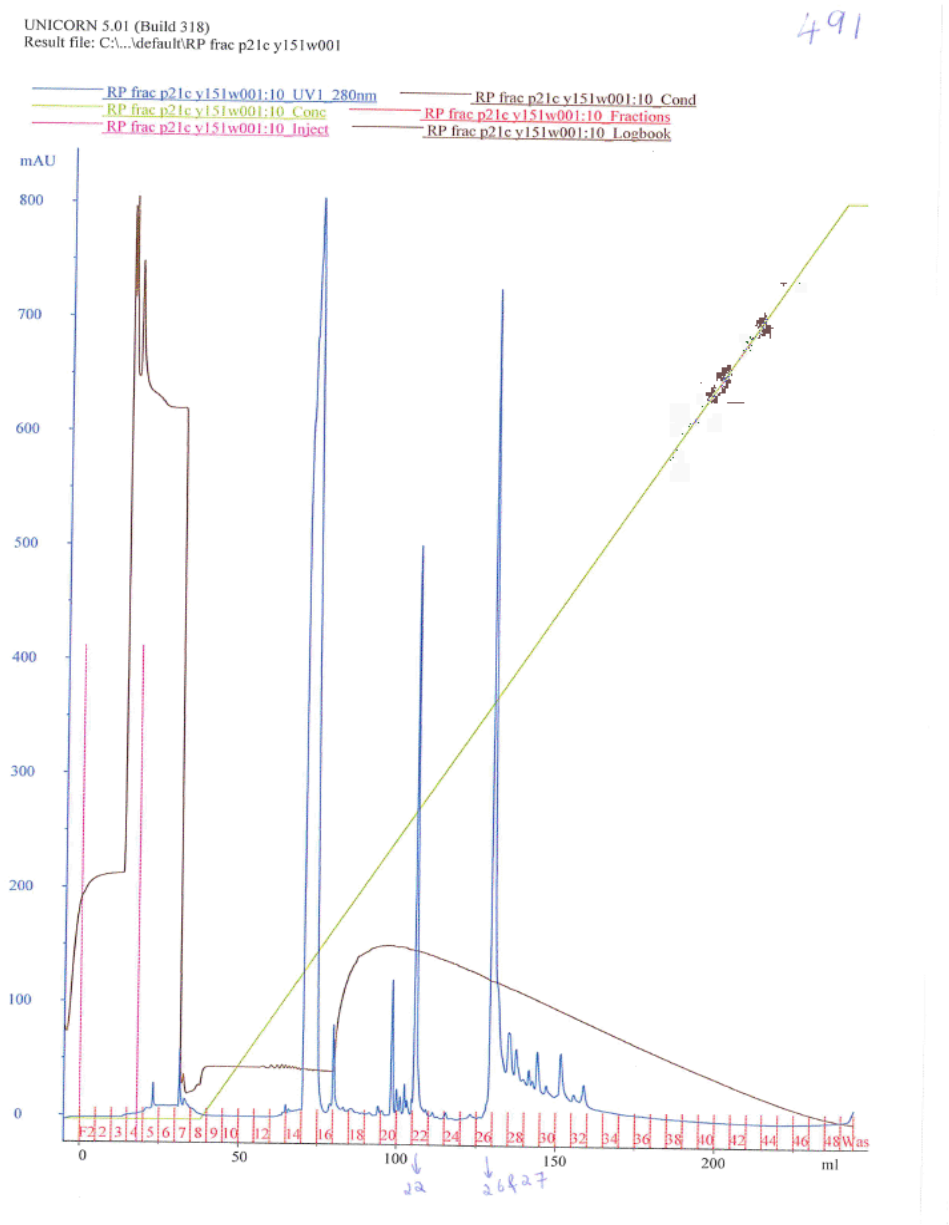

Figure 8. Reversed Phase Chromatogram of p21CY151W mutant. The eluent A used was 0.1% trifluroacetic acid (TFA) and eluent B was 0.1% TFA and 100% acetonitrile (ACN). The flow rate maintained was 2 ml/min at 25^0C and protein was monitored by absorbance at 280 nm. The p21CY151W mutant after thrombin digestion bound to the C18 column and eluted at the 22^{nd} fraction (as shown by subsequent mass spectrometry analysis) and the lipo part in the 26^{th} and 27^{th} fraction. The brown curve shows the base line conductivity. The green curve shows the gradient obtained by increasing eluent B concentration gradually. The blue curve shows the absorbance at 280 nm.

4.2.5. Reversed phase chromatography of p21C:

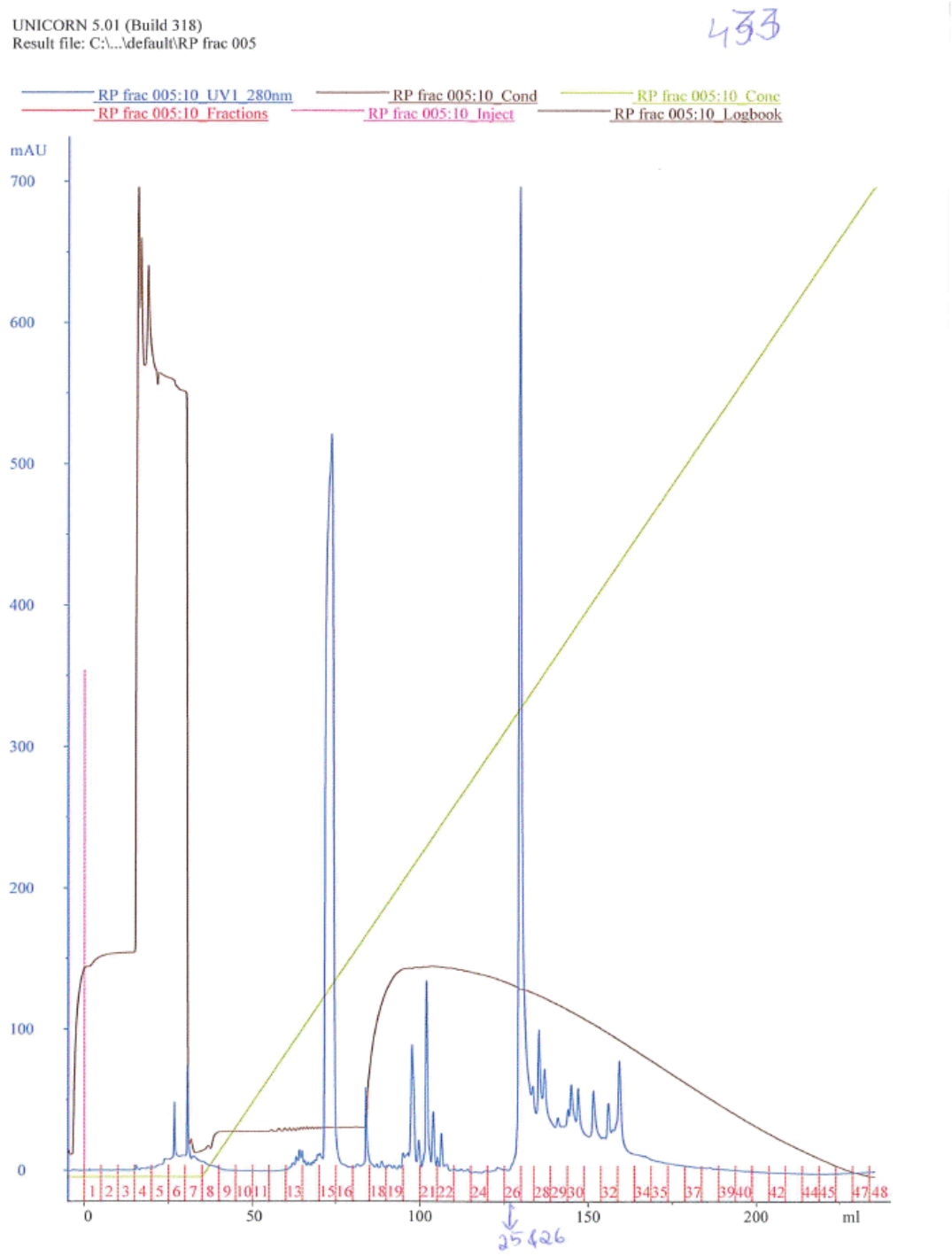

Figure 9. Reversed phase chromatogram of p21C. The eluent A used was 0.1% trifluroacetic acid (TFA) and eluent B was 0.1% TFA and 100% acetonitrile (ACN). The flow rate maintained was 2 ml/min at 25^0C and the protein absorbance was measured at 280 nm. The p21C peptide fragment after thrombin digestion bound to the C18 column and collected in the 21st fraction and lipo part in the the 25th and 26th fraction (due to improper thrombin digestion, some of the peptide was eluted along with the lipo part). The brown curve shows the base line conductivity. The green curve shows the linear gradient set by gradual increase in eluent B volume. The blue curve shows the absorbance at 280 nm.

4.2.6. Anion exchange chromatography of HPV45 E7C:

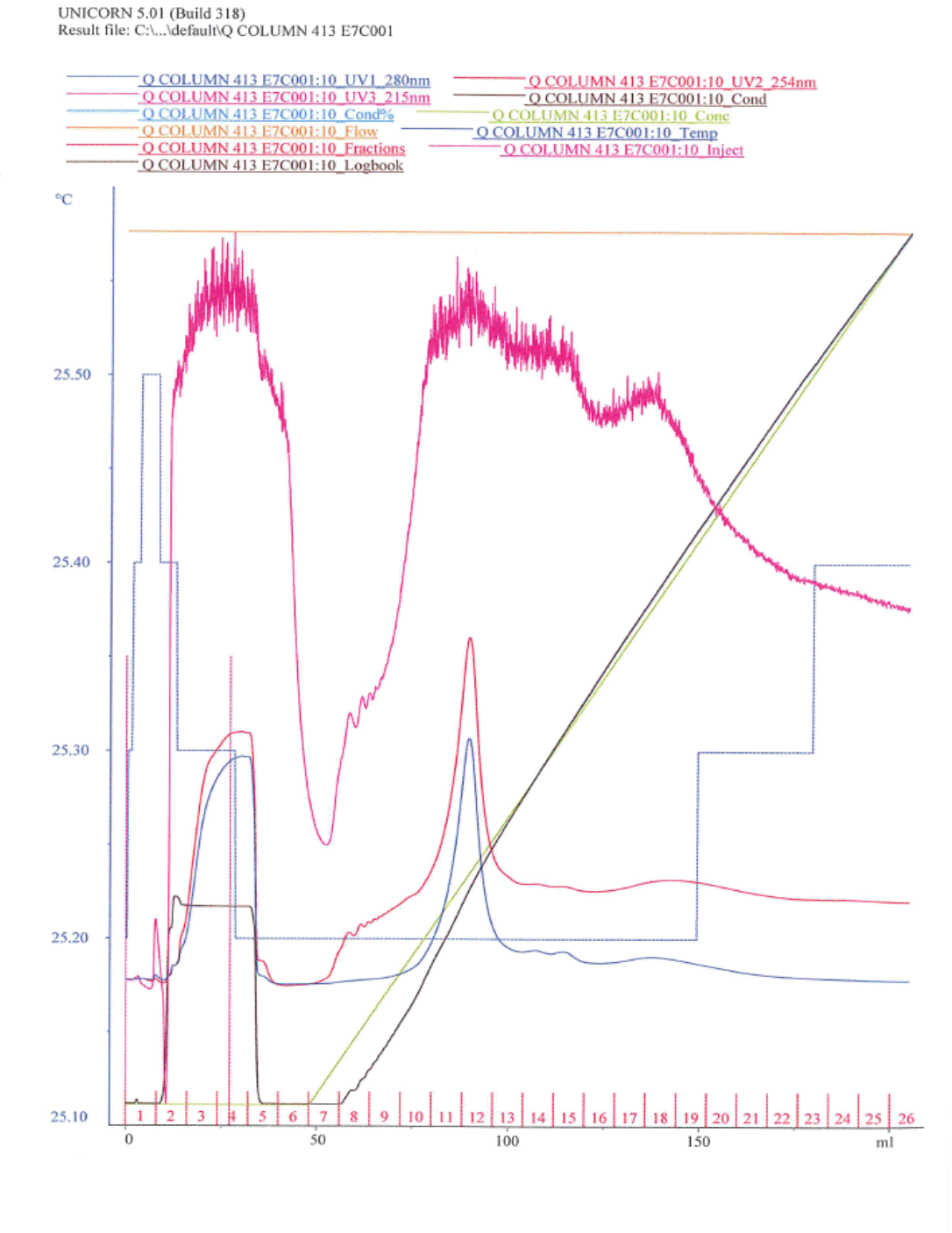

Figure 10. Q column chromatogram of HPV45 E7C. The HPV45 E7C protein was bound to the column and collected in the 11th and 12th fraction respectively with a 0-100% gradient of 2 M NaCl. The black curve indicates the base line conductivity. The green curve indicates the concentration gradient set using the buffer B. The blue curve indicates the absorbance at 280 nm. The red curve indicates the absorbance at 215 nm. The eluent A used was 50 mM Tris pH 8.5, 2 mM Mercaptoethanol and the eluent B was 50 mM Tris pH 8.5, 2 mM Mercaptoethanol with 2 M NaCl . The flow rate maintained was 2 ml/min at 25^{0}C.

4.2.7. Mass spectrometry analysis of the p21C showing the peptide fragment:

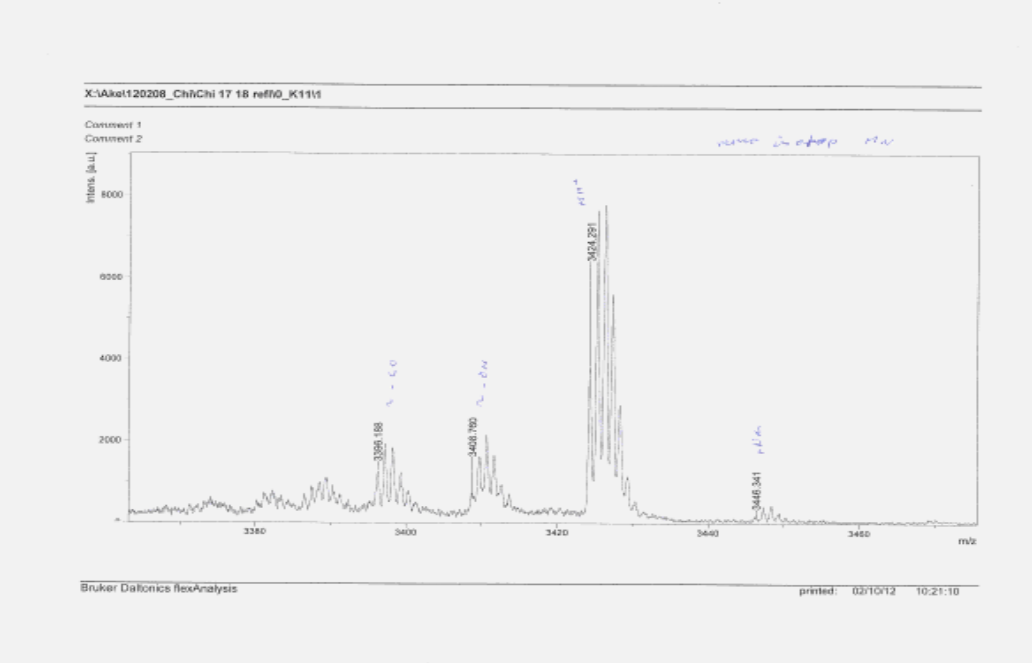

Figure 11. Mass spectrometry of p21C wildtype showing that the peptide fragment G S G R K R R Q T S M T D F Y H S K R R L I F S K R K P has been cleaved after thrombin digestion and the corresponding peak is observed at a m/z ratio of 3424.291 with respect to its molecular weight.

4.2.8. Mass spectrometry analysis of the lipo part of p21C:

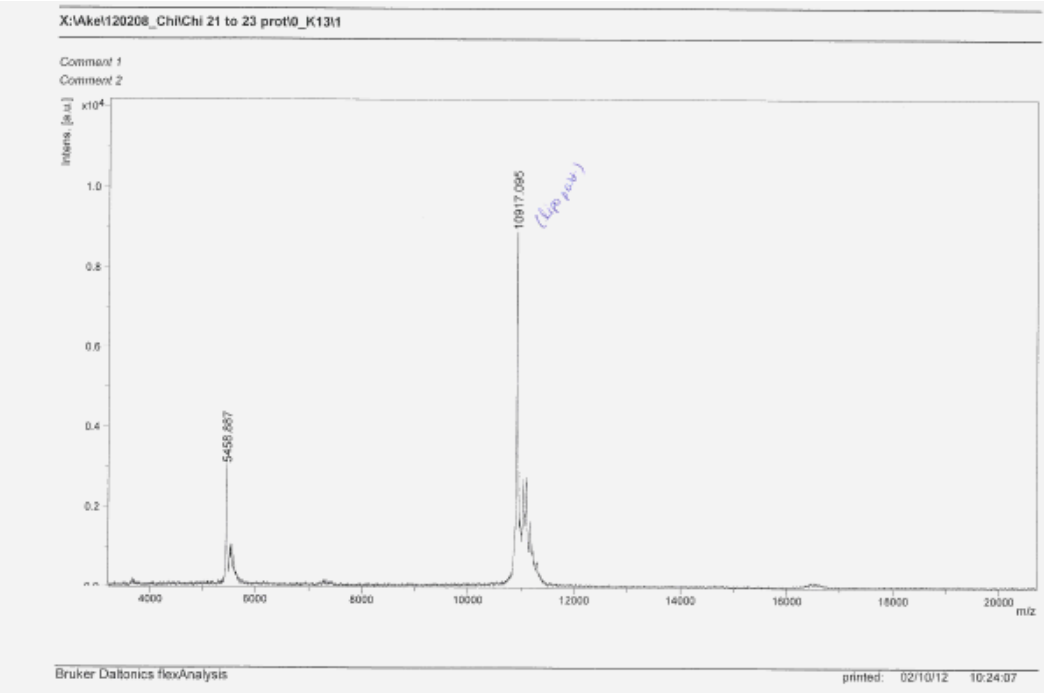

Figure 12. Mass spectrometry of p21C wildtype showing that the lipo part of the protein is cleaved after thrombin digestion and a corresponding peak is observed at an m/z ratio of 10917.095 with respect to its molecular weight.

4.3. Stability studies:

Equilibrium denaturation experiments were conducted for HPV45 E7F, HPV45 E7C in 0.3 M sodium sulfate, HPV16 E7F and the solubilized form of HPV16 E7F in 4 M urea. The measured fluorescene intensity was plotted against the denaturant i.e. guanidine hydrochloride and fitted into a solvent denaturation equation (32). It shows that HPV45 E7F and HPV45 E7C in 0.3 M sodium sulfate were properly folded through the sigmoidal curve (Figure 13). Equilibrium experiment for the natively purified HPV16 E7F and HPV16 E7F solubilized in 4 M urea suggested that unfolding results upon increasing the GdnHCl concentration and both the proteins had a similar sigmoidal denaturation curve (Figure 14). The experiment thus suggests that the two E7F preparations display a similar change in solvent-accessible surface area upon denaturation due to similar $m_{D\text{-}N}$ values (Table 2). Circular dichroism spectra were generated by plotting the molar ellipticity against the emission wavelength for the native proteins HPV45 E7C, HPV45 E7F and p21C at 25^0C (Figure 15). Attempts were made to disturb the native state of the protein HPV45 E7F by raising the temperature (melting) from 4^0C till 70^0C and recording the CD signal at 210 nm. Unfolding of E7F starts around 50^0C and got completed at 70^0C (Figure 16). Circular dichroism spectra were generated for the HPV45 E7F sample with and without heat treatment. Heat treatment was performed by raising the temperature to 80^0C and then cooling the sample. Spectra for both the samples of E7F were recorded at 25^0C. The similar spectra show that E7F has similar secondary structure before and after heating (Figure 17).

4.3.1. Guanidine Hydrochloride denaturation of HPV45 E7F and HPV45 E7C in 0.3 M sodium sulfate:

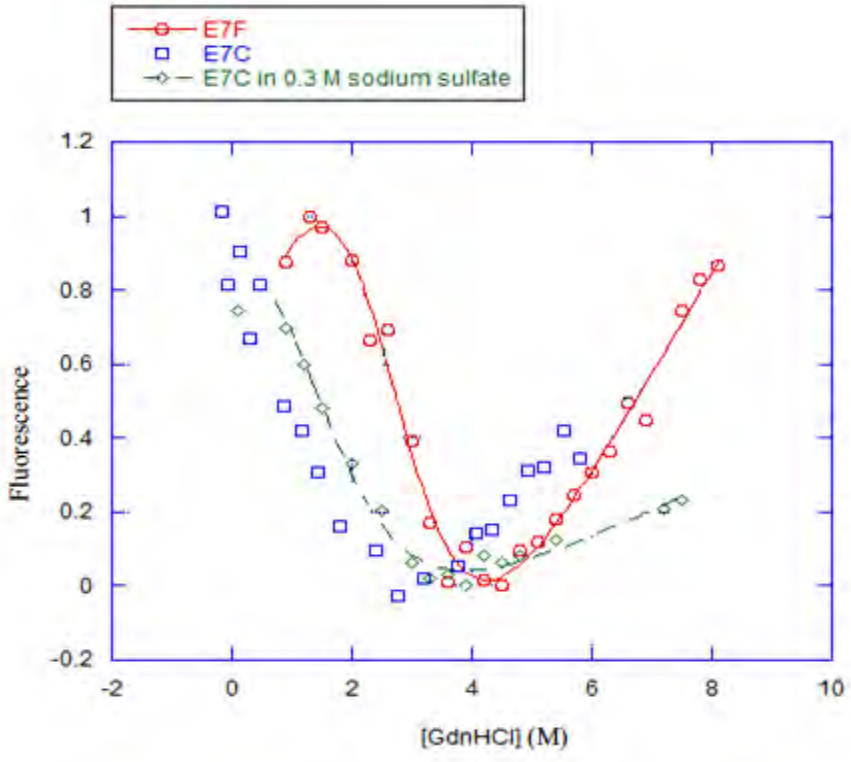

Figure 13. Graphical representation of the stability analysis of HPV45 E7F, HPV45 E7C in 0.3 M sodium sulfate and HPV16 E7C showing the fluorescence (normalized values) on the y axis plotted against the guanidine HCl concentration (in M) on the x axis. Emission was monitored at wavelength of 335 nm after excitation at 280 nm.

Protein	m_{D-N} value. kcal $mol^{-1}M^{-1}$	$[Urea]_{50\%}$ M	$\Delta G_{D-N}H_2O$ kcal mol^{-1}
E7F	0.9±0.1	2.6 ± 0.2	2.2±0.4
E7C in 0.3 M sodium sulfate	0.9±0.4	1.5±0.1	1.3±0.6

Table.1. Parameters for equilibrium denaturation experiments of HPV45 E7F and HPV45 E7C in 0.3 M sodium sulfate.

4.3.2. Guanidine Hydrochloride denaturation of HPV16 E7F and HPV16 E7F in 4 M urea:

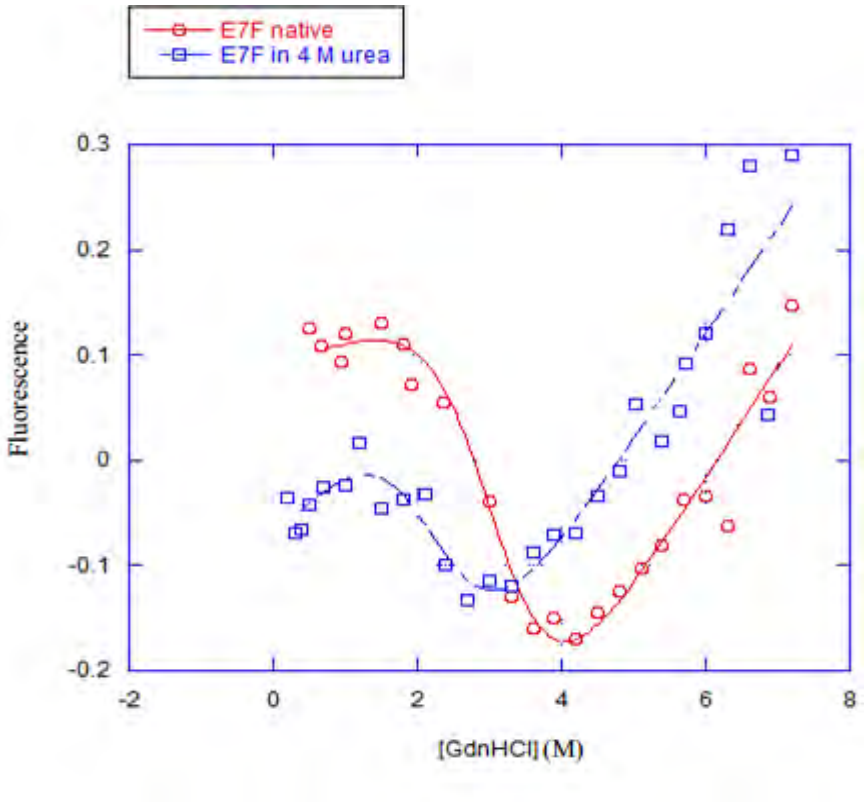

Figure 14. Graphical representation of the stability analysis of HPV16 E7F and HPV16 E7F solubilised in 4 M urea showing the fluorescence (normalized values) on the y axis plotted against the guanidine HCl concentration (in M) on the x axis. Emission was monitored at wavelength of 335 nm after excitation at 280 nm.

Protein	m_{D-N} value. kcal $mol^{-1}M^{-1}$	$[Urea]_{50\%}$ M	$\Delta G_{D-N}H_2O$ kcal mol^{-1}
E7F native	1.2±0.2	3.1 ± 0.2	3.9±0.9
E7F in 4 M urea	1.2±0.2	2.3±0.1	2.7±0.5

Table.2. Parameters for equilibrium denaturation experiments of HPV16 E7F native and HPV16 E7F in 4 M urea.

4.3.3. Circular dichroism spectra of HPV45 E7C, HPV45 E7F and p21C:

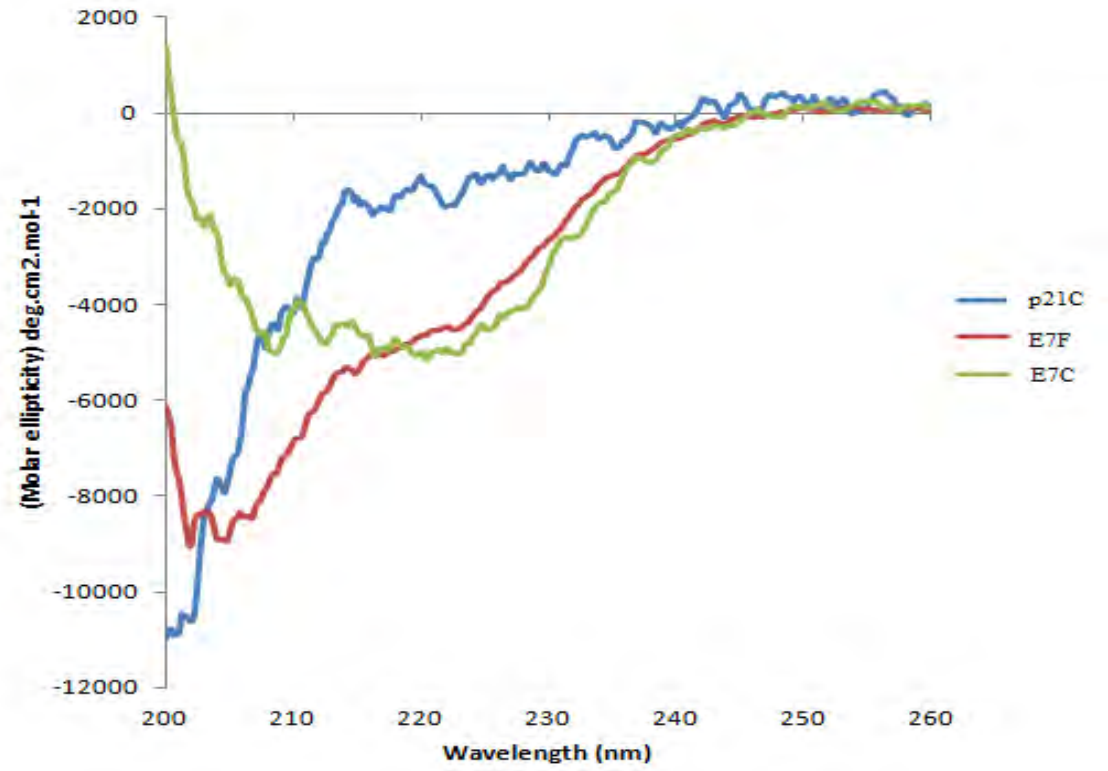

Figure 15. The blue spectrum shows the molar ellipticity of the protein p21C. The red spectrum shows the molar ellipticity of the protein E7F. The green spectrum shows the molar ellipticity of the peptide E7C.

4.3.4. CD signal of HPV45 E7F at 210 nm:

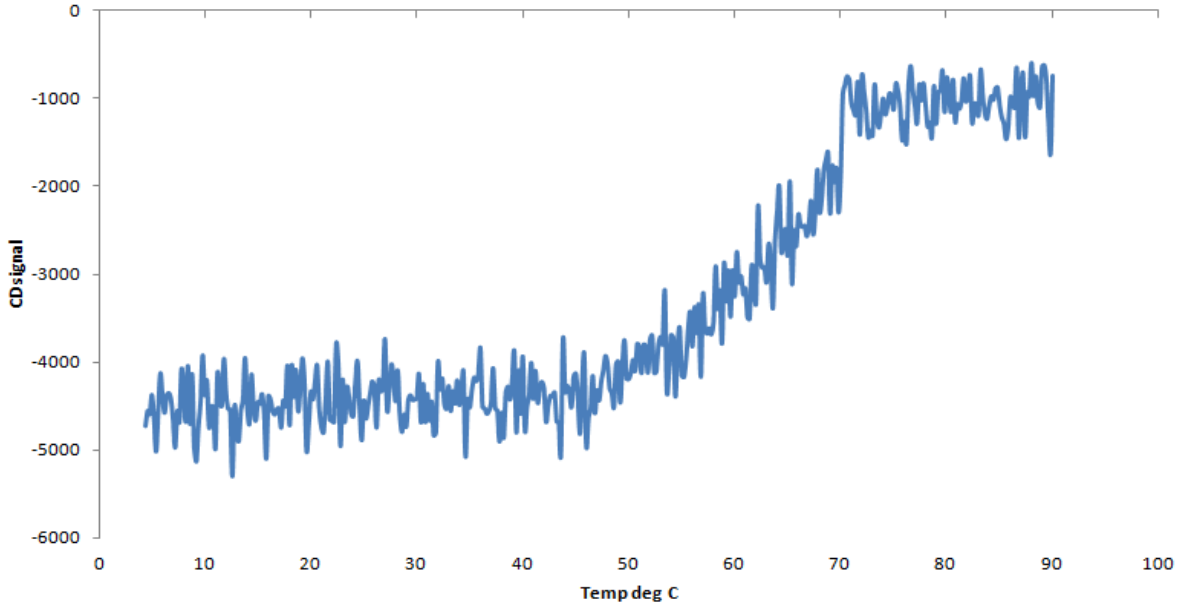

Figure 16. CD signal at 210 nm for HPV45 E7C melting from 4^0C till 90^0C.

4.3.5. Circular dichroism spectra of HPV45 E7F before and after thermal denaturation:

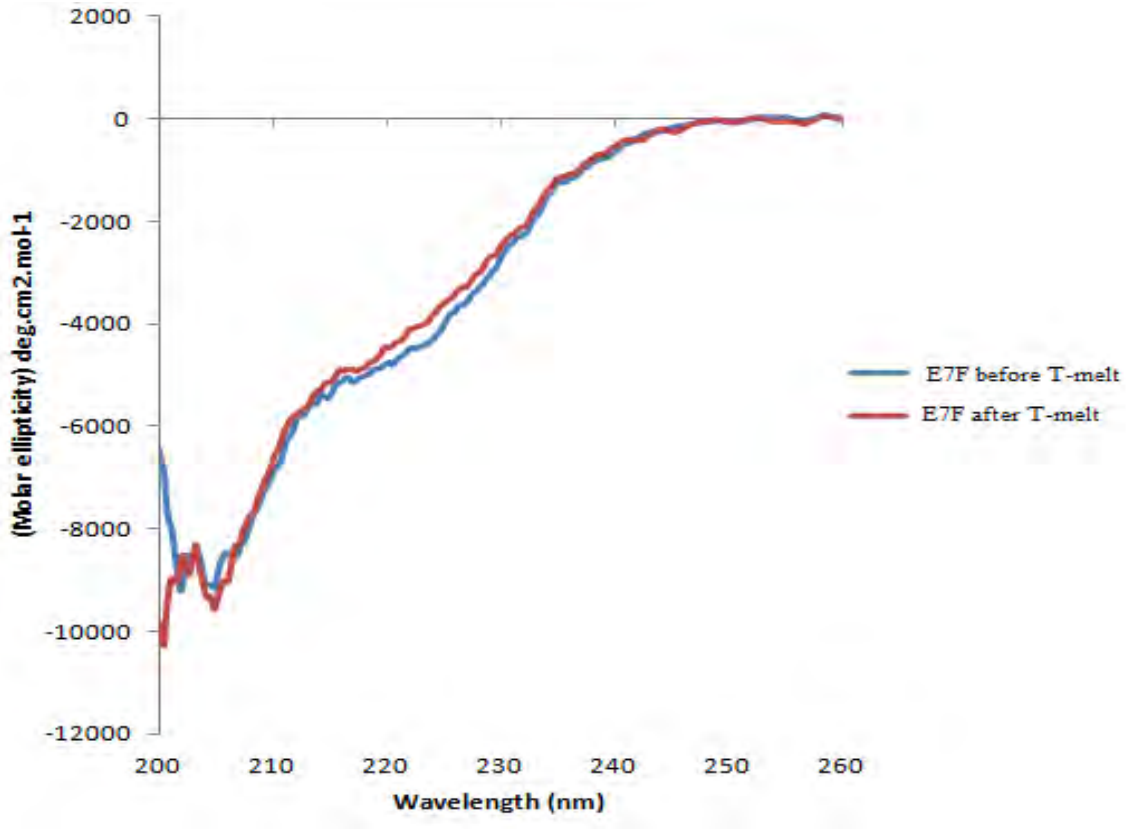

Figure 17. The blue spectrum shows the E7 full length protein molar ellipticity. The red spectrum shows the molar ellipticity of E7 full length after heating at 80^0C followed by cooling. The concentration of the E7C protein and p21C peptide was made to be 25 μM in 50 mM potassium phosphate and the spectra were recorded at 25^0C.

4.4. Binding studies:

Binding studies were conducted for E7F and p21C at constant E7F protein concentration (1 μM) and by varying the p21C concentration. The proteins used for binding were in 50 mM potassium phosphate buffer at pH 7.4 and experiments were conducted at 37^0C and 10^0C. Biphasic behaviour was observed for the binding, suggesting that the binding may follow either an induced fit or a conformational selection type of scheme (Figure 18 & 19).

4.4.1. Binding kinetics of E7F and p21C at 37^{0}C:

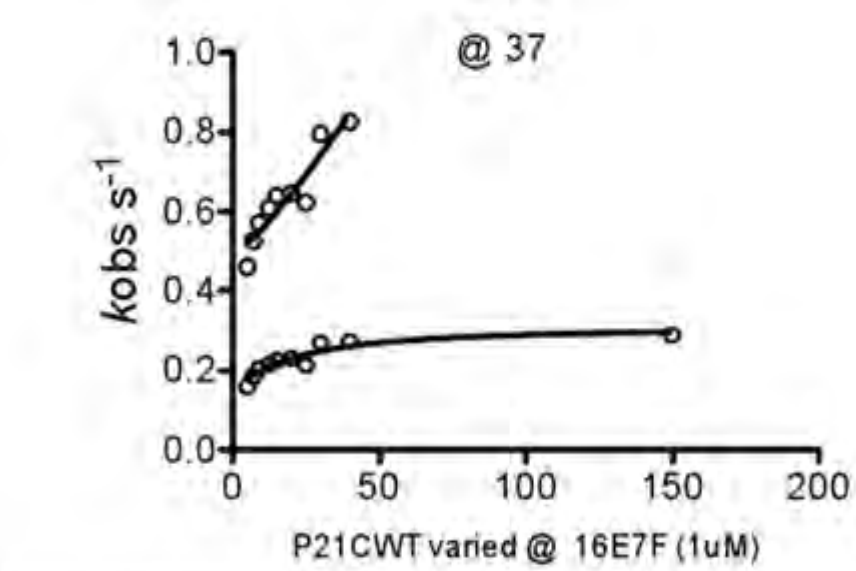

			Global (shared)
k1	0.01168	0.01168	0.01168
k2	0.3260	0.3260	0.3260
k3	0.08413	0.08413	0.08413
k4	0.2270	0.2270	0.2270

			Global (shared)
k1	0.3111	0.3111	0.3111
k2	0.1732	0.1732	0.1732
k3	0.01168	0.01168	0.01168
k4	0.1528	0.1528	0.1528

Figure 18. Binding kinetics of HPV16 E7F showing the observed rate constant of binding plotted against various concentrations of p21C WT at 37^{0}C. The fitted parameters in the left box are for induced fit and those in the right box are for conformational selection.

4.4.2. Binding kinetics of E7F and p21C at 10^{0}C:

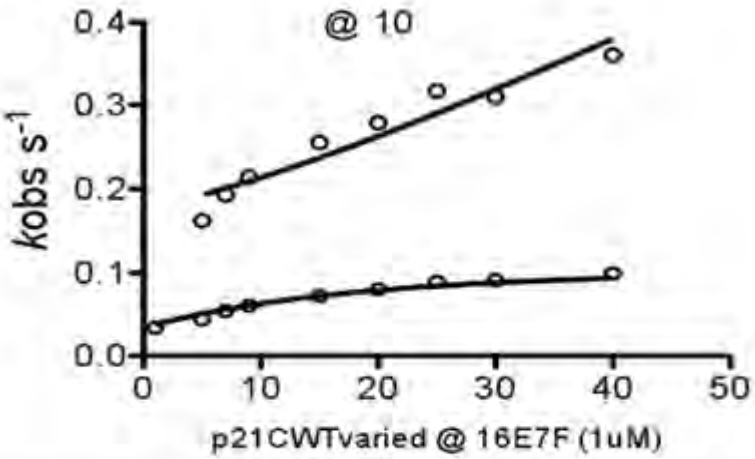

			Global (shared)
k1	0.006538	0.006538	0.006538
k2	0.09911	0.09911	0.09911
k3	0.05041	0.05041	0.05041
k4	0.06163	0.06163	0.06163

			Global (shared)
k1	0.1120	0.1120	0.1120
k2	0.06451	0.06451	0.06451
k3	0.006538	0.006538	0.006538
k4	0.03459	0.03459	0.03459

Figure 19. Binding kinetics of HPV16 E7F showing the rate constant of binding plotted against various concentrations of p21C WT at 10^{0}C. The fitted parameters in the left box are for induced fit and those in the right box are for conformational selection.

5. Discussion:

We successfully cloned and expressed the constructs for HPV16 E7F, HPV45 E7F, HPV45 E7C, p21F, p21C and mutants of the HPV45 E7 and p21 constructs. In order to understand the mechanism of binding interaction of E7 with the tumor suppressor p21, mutations were created in HPV45 E7 and p21 involving tryptophan residues, since we wanted to use tryptophan as a probe to monitor binding and stability of the protein. We further proceeded to express and purify the wild types and the constructs which contained tryptophan mutations for further studies. We purified the protein to near homogeneity using affinity purification followed by further purification by anion exchange and reversed phase chromatographic techniques. We also determined the stability of the E7 construct purified under native conditions and in the presence of urea. We found that E7 purified under both native and in the presence of urea unfold upon denaturation through addition of a chemical agent *i.e.* GdnHCl or by rising the temperature as judged from the fluorescence and circular dichroism measurements. Our preliminary results on binding kinetics at different temperatures indicate that E7 interacts with p21 through a minimum of two steps.

The binding studies were performed between the wild types of HPV16 E7F and p21C at two different temperatures 10^0C and 37^0C. By varying p21C with fixed HPV16 E7F concentration the binding traces were biphasic and hence the data were fitted into a double exponential function to find the rate constants- k_{obs1} and k_{obs2} (34). A biphasic reaction implies at least a two step binding *i.e.* induced fit or conformational selection.

Induced fit is the one which occurs through the following way *i.e.* equilibrium occurs rapidly followed by a slow conformational change as follows i.e. $k_2 >> k_3$

$$E7 + p21 \underset{k_1}{\overset{k_2}{\leftrightharpoons}} E7\ p21 \underset{k_3}{\overset{k_4}{\leftrightharpoons}} E7\ p21^{*} \text{--->Equation 4}$$

The dependence on the off rate constants (k_2 and k_4), on rate constant k_1 and intramolecular rate constant k_3 are related with observed rate constants k_{obs1} and k_{obs2} for the two steps as follows:

$k_{obs1}=k_2[p21] + k_1$

$k_{obs2}=k_3 + k_4[p21]/(K+[p21])$,thus k_{obs2} will increase hyperbolically with increasing p21 concentration.

Conformational selection is the other mechanism in which the protein exists in different conformations and the ligand binds with one of them.

$$E7+p21 \underset{k_1}{\overset{k_2}{\leftrightharpoons}} E7^{*}+p21^{*} \underset{k_3}{\overset{k_4}{\leftrightharpoons}} E7p21^{*} \text{--->Equation 5}$$

The on and off rate constants are related with the observed rate constants as

$k_{obs1}=k_4 + k_3[p21]$

$k_{obs2}=k_2+k_1[p21]/(K+[p21])$, k_{obs2} will also increase hyperbolically with increasing p21 concentration. K is the equilibrium dissociation constant which is a measure of binding affinity between E7 and p21, $K=k_4/k_3(k_{off}/k_{on})$.

The observed rate constant measured was plotted against the concentration of the varied species p21. The rate constants were found to be well fitted for both the induced fit and the conformational selection mechanisms. The k_1 values corresponding to the slope of the graph and k_2 values corresponding to the intercept were found to be higher for higher temperature binding experiments *i.e.* at 37^0C. There was a three time increase in the slope and intercept at 37^0C when compared at 10^0C. The observed kinetic data suggest that it could follow an induced fit or a conformational selection but the exact mechanism of interaction will be known if the concentration of the other reacting species i.e. E7 is varied by keeping p21C concentration to be constant and plotting the values of the observed rate constant against E7 concentration.

HPV16 E7F got precipitated after purification, so we purified it by adding solubilising agent *i.e.* 4 M urea. The natively purified E7 and E7 purified with 4 M urea were both folded, as revealed by the sigmoidal curves with similar $m_{D\text{-}N}$ values resulting from GdnHCl denaturation. Far UV dichroism spectra of HPV16 E7F, HPV45 E7C and p21C suggested that 1) all E7 had similar secondary structures, 2) the p21C was highly unfolded and had a random coil structure and 3) E7F got unfolded completely at 70^0C and found to have similar CD spectrum as other E7 proteins upon cooling.

6. Conclusion:

We observed a biphasic kinetic mechanism of interaction between HPV16 E7F and p21C binding. The observed rate constants could be fitted to an induced fit or conformational selection mechanism. There was no considerable difference in the folding for the protein HPV16 E7F in its native state and the state purified using urea. This suggests that urea can be added during the purification of HPV16 E7F.

Future Perspectives:

We further aim to study the binding kinetics for the respective mutants of the HPV16 E7F with p21 by creating mutations in the residues that form a part of the interface of the binding. We also would like to understand the conformation of this protein *i.e.* whether it exist as a dimer, monomer or an equilibrium mixture of all the possible states. This will be achieved through gel filtration.

Acknowledgement:

Foremost, I would like to express my sincere gratitude to Dr. Per Jemth for giving me an opportunity to do my master thesis in his lab. I would like to thank my supervisors Dr. Per Jemth and Dr. Celestine Chi for their constant guidance, support, motivation and encouragement throughout my thesis. Finally I thank my labmates for all their support and all the fun we have had for the last 5 months.

References:

1. Evans, T., Rosenthal, E., Youngbloom, J.,Distel, D. and Hunt, J. (1983), *Cell* **33**: 389-396.

2. Adkins, H. B., S. C. Blacklow, and J. A. Young. (2001). Two functionally distinct forms of a retroviral receptor explain the nonreciprocal receptor interference among subgroups B, D, and E avian leukosis viruses. *J. Virol*. **75**: 3520-3526.

3. Ferlay J., Bray F., Pisani P., Parkin D.M. Globocan (2000). Cancer incidence, mortality and prevalence worldwide, version 1.0. IARC CancerBase no. 5. Lyons, France: IARC Press, 2001.

4. De Villiers E-M. (2001) Taxonomic classification of papillomaviruses. *Papillomavirus Rep*; **12**: 57-63

5. Jacobs M.V., De Roda Husman A.M., Van den Brule A.J.C., Snijders P.J.F., Meijer C.J.L.M., (1995) Walboomers J.M.M. Group-specific differentiation between high- and low-risk human papillomavirus genotypes by general primer-mediated PCR and two cocktails of oligonucleotide probes. *J Clin Microbiol*; **33**: 901-905

6. Van den Brule A.J., Pol R., Fransen-Daalmeijer N., Schouls L.M., Meijer C.J.L.M., Snijders P.J. (2002). GP5+/6+ PCR followed by reverse line blot analysis enables rapid and high-throughput identification of human papillomavirus genotypes. *J. Clin Microbiol*; **40**: 779-787

7. Doorbar J. (2005). The papillomavirus life cycle; *J Clin Virol*; **32**: 7-15

8. Jo and Kim J. W. (2005). Implications of HPV infection in uterine cervical cancer; *Cancer Ther.* **3**: 419-434.

9. Thorland E. C., Myers S. L., Gostout B. S. and Smith D. I. (2003). Common fragile sites are preferential targets for HPV16 integration in cervical tumours, *Oncogene* **22**: 1225-1237.

10. Jeon S. and Lambert P. F. (1995) Integration of human papilloma virus type 16 DNA into the human genome leads to increased stability of E6 and E7 mRNAs: implications of cervical carcinogenesis; *Proc. Natl. Acad. Sci.* **92**: 1654-1658.

11. Karl M., Amy B., Kirsten M. Edwards, Hiroyuki H., Christine L., Nguyen., Michael O., Miranda G. and Kyung Won H. (2004). Mechanisms of Human Papillomavirus-Induced Oncogenesis; *J.Virol.* **28**: 11451-11460.

12. Mungler K. and Howley P. M. (2002). Human papillomavirus immortalization and transformation function; *Virus res*, **89**: 213-228.

13. Dyson N., Howley P. M., Munger K. and Harlow E. (1989). The human papillomavirus 16 E7 oncoprotein is able to bind to the retinoblastoma gene product; *Science* **17**: 934-937.

14. Liu X., Clements A., Zhao K. and Marmorstein R. (2006). Structure of the human papillomavirus E7 oncoprotein and mechanism for inactivation of the retinoblastoma tumor suppressor; *J. Biol. Chem*. **281**: 578-586.

15. Funk J. O., Waga S., Harry J. B., Espling E., Stillman B. and Galloway D. A. (1997). Inhibition of CDK activity and PCNA dependent DNA replication by p21 is blocked by interaction with HPV 16E7 oncoprotein; *Genes Dev*. **11**: 2090-2100.

16. Zerfass-Thome K., Zwerschke W., Manhadrdt B., Tindle R., Botz J. W. and Jansen Durr P. (1996). Inactivation of the CDK inhibitor p27K1P1 by the human papillomavirus type 16 E7 oncoprotein; *Oncogene* **13**: 2323-2330.

17. Barbosa, M. S., Lowy, D. R., and Schiller, J. T. (1989). Papillomavirus polypeptides E6 and E7 are zinc- binding proteins,*J. Virol*. **63**: 1404-1407.

18. MaIntyre, M. C., Frattini, M. G., Grossman, S.R., and Laimins, L. A. (1993). Human papillomavirus type 18 E7 protein requires intact Cys-X-X-Cys motifs for zinc binding, dimerization, and transformation but not for Rb binding. *J. Virol*. **67**: 3142-3150.

19. Chen, J., P.K. Jackson, M.W. Kirschner, and A. Dutta. (1995). Separate domains of p21 involved in the inhibition of cdk kinase and PCNA. *Nature* **374**: 386-388.

20. Luo, Y., J.Hurwitz, and J. Massague. (1995). Cell cycle inhibition mediated by functionally independent CDK and PCNA binding domains in $p21^{C1P1}$.*Nature* **375**: 159-161.

21. Nakanishi, M., R.S. Robetorge, O.M. Pereira-Smith, and J.R.Smith. (1995). The carboxy-terminal region of $p21^{SD11/WAF1/C1P1}$ is involved in proliferating cell nuclear antigen binding but does not appear to be required for growth inhibition. *J. Biol. Chem*. **270**: 17060-17063.

22. Chen, J., P. Saha, S. Kornbluth, B. D. Dynlacht, and A.Dutta. 1996. Cyclin binding motifs are essential for the function of $p21^{C1P1}$.*Mol. Cell. Biol.* **16**: 4673-4682.

23. Ogryzko, V.V., P. Wong and B. H. Howard. (1997). WAF1 retards S-phase progression primarily by inhibition of cyclin-dependent kinases. *Mol. Cell. Biol.* **17**: 4877-4882.

24. Adams, P.D., W.R. Sellers, S.K. Sharma, A.D. Wu, C.M. Nalin, and W.G. Kaelin. (1996). Identification of a cyclin-cdk2 recognition motif present in substrates and p21-like cyclin-dependent kinase inhibitors. *Mol. Cell. Biol*. **16**: 6623-6633.

25. Ball, K.L., S. Lain, R.Fahraeus, C.Smythe, and D.P.Lane . (1996). Cell-cycle arrest and inhibition of cdk4 activity by small peptides based on the carboxy-terminal domain of $p21^{WAF1}$. *Curr. Biol*. **7**: 71-80.

26. Chen, J., P. Saha, S. Kornbluth, B.D. Dynlacht, and A.Dutta. (1996). Cyclin-binding motifs are essential for the function of $p21^{C1P1}$. *Mol.Cell. Biol*. **16**: 4673-4682. 28

27. Li, R., S. Waga, G.J. Hannon, D. Beach, and B. Stillman. (1994). Differential effects by the p21 CDK inhibitor on PCNA dependent DNA replication and repair. *Nature* **371**: 534-537.

28. Waga, S., G.J. Hannon, D. Beach, and B. Stillman. (1994b). The p21 inhibitor of cyclin-dependent kinases controls DNA replication by interaction with PCNA. *Nature* **369**: 574-578.

29. Jens Oliver F., Shou W., Jo Beth H, *et al*.(1997) Inhibition of CDK activity and PCNA-dependent DNA replication by p21 is blocked by interaction with the HPV-16 E7?oncoprotein. *Genes Dev.* **11:** 2090-2100.

30. Jones, D. L., D. A. Thompson and K.Munger. (1997). The human papillomavirus E7 oncoprotein can uncouple cellular differentaition and proliferation in human keratinocytes by abrogating p21Cip-mediated inhibiton of cdk2. *Genes Dev*. **11**: 2101-2111.

31. Ranjbar, B., Pooria, G. (2009). Circular dichroism techniques: Biomolecular and nano structural analyses- a review. *Chem Biol Drug Des*. **74**: 101–120.

32. Fersht, A. (1999). Structure and mechanism in protein science: A guide to enzyme catalysis and protein folding (Newyork, Freeman).

33. Jang D.J., Sayed M. A. (1989). Tryptophan fluorescence quenching as a monitor for the protein conformation changes occurring during the photocycle of bacteriorhodopsin under different perturbations. *Proc Natl Acad Sci U S A.* **86**: 5815-5819.

34. Chi C.N., Bach A., Engström Å., Wang H., Strømgaard K., Gianni S., Jemth P. (2009). *Biochemistry* **48:** 7089–7097

Appendix I:

PCR Master mix contents

S.No	PCR Reaction mix
1	5µl 10X Pfu Ultra buffer
2	2.5µl dNTP
3	0.5µl DMSO
4	1µl template
5	1.5 µl forward primer
6	1.5 µl reverse primer
7	0.5 µl Pfu enzyme

The final volume was made upto 50 µl with distilled water.

Appendix II:

PCR cycle parameters

Step	Temperature	Duration	Cycles
Heated lid	111°C		
Hot start (Automatic)	95°C	2 min	1
Denaturation	94°C	30 sec	35
Annealing	60°C	30 sec	35
	61°C	30 sec	35
	62°C	30 sec	35
	64°C	30 sec	35
Elongation	72°C	3.30 min	35
Final Elongation	72°C	10 min	1
Store	4°C	∞	1

Appendix III:

SDS PAGE Gel Composition

Stacking Gel	Separating Gel (15%)
H_2O-3000µl	H_2O-1190µl
Glycerol(80%) –No	Glycerol(80%) -1250µl
Tris HCl pH6.8, 0.4%SDS-1250 µl	Tris HCl pH8.8, 0.4%SDS-2500µl
Acrylamide(30%)-750 µl	Acrylamide(30%)-5000 µl
APS(40%)-8 µl	APS(40%)-30 µl
TEMED- 8 µl	TEMED- 30 µl
Total volume=5000 µl	Total volume=10000 µl

Stain Solution Composition:

0.15% CBS(Coomassie brilliant blue) R250

10% Acetic acid

25% Isopropanol

Destaining Solution:

10% Acetic acid

10% Isopropanol